

1 **Effects of Urbanization on the water cycle in the Shiyang River**

2 **Basin: Based on stable isotope method**

3 Rui Li^{a,b}, Guofeng Zhu^{a,b,*}, Siyu Lu^{a,b}, Liyuan Sang^{a,b}, Gaojia Meng^{a,b}, Longhu Chen^{a,b},

4 Yinying Jiao^{a,b}, Qinqin Wang^{a,b}

5 **Affiliations:**

6 ^a *College of Geography and Environmental Science, Northwest Normal University, Lanzhou*

7 *730070, Gansu, China*

8 ^b *Shiyang River Ecological Environment Observation Station, Northwest Normal University,*

9 *Lanzhou 730070, Gansu, China*

10 **Corresponding author. Email: zhugf@nwnu.edu.cn.*

11 **Abstract:** In water-scarce arid areas, the water cycle is affected by urban

12 development and natural river changes, and urbanization has a profound impact on the

13 hydrological system of the basin. Through an ecohydrological observation system

14 established in the Shiyang River basin in the inland arid zone, we studied the impact

15 of urbanization on the water cycle of the basin using isotope methods. The results

16 showed that urbanization significantly changed the water cycle process in the basin,

17 and accelerated the rainfall-runoff process due to the increase of urban land area, and

18 the mean residence time (MRT) of river water showed a fluctuating downward trend

19 from upstream to downstream, and was shortest in the urban area in the middle

20 reaches, and the MRT was mainly controlled by the landscape characteristics of the

21 basin. In addition, our study showed that river water and groundwater isotope data

22 were progressively enriched from upstream to downstream due to the construction of

23 metropolitan landscape dams, which exacerbated evaporative losses of river water,

24 and also strengthened the hydraulic connection between groundwater and river water
25 around the city. Our findings have important implications for local water resource
26 management and urban planning and provide important insights into the hydrologic
27 dynamics of urban areas.

28 **Keywords:** Urbanization; Water cycle; Stable isotopes; River Connectivity

29 **1 Introduction**

30 According to the "2020 Global Cities Report," urban areas are currently home to
31 more than half of the worldwide people, which amounts to 56.2%. This pattern is
32 expected to continue over the course of the next decade, culminating in an
33 urbanization rate of 60.4% by the year 2030. In addition, the study forecasts that by
34 the year 2050, approximately seventy percent of the world's population would reside
35 in urban areas (Chen et al., 2020; UN, 2019; UN-Habitat, 2020). Unlike other regions,
36 urban regions have a substantial influence on the hydrological system, resulting in
37 significant consequences on water balance and the water cycle (Gillefalk et al., 2021).
38 To meet the diverse household and industrial requirements in metropolitan areas,
39 where the population is concentrated and water demands are high, a complex
40 interplay between natural and manmade components of the water cycle is required.
41 These components include both natural features such as streams and groundwater, as
42 well as human-made systems like drinking water and drainage networks (Gessner et
43 al., 2014). Urbanization exacerbates water depletion and has far-reaching impacts on
44 groundwater (Flörke et al., 2018; McDonough et al., 2020), affecting the environment
45 and water availability (Bhaskar and Welty, 2015). Rapid urbanization will seriously

46 pressure the structure, function and water quality degradation of basin ecosystems
47 (Grimm et al., 2008; Sun and Lockaby, 2012; Sun et al., 2015).

48 Urbanization's effects on basin hydrology and the related processes have
49 complex and varying consequences (Caldwell et al., 2012; Martin et al., 2017). In the
50 past few decades, with the continuous acceleration of urbanization, human activities
51 in urban areas have become more frequent, and the hydrological effects of
52 urbanization have become more intense, attracting widespread attention worldwide
53 (Salvadore et al., 2015). The rise of impervious rivers in urbanized regions increases
54 the rate of urban water runoff, which raises the danger of urban floods (Wing et al.,
55 2018). In addition, high-intensity human activities have led to increased discharge of
56 domestic sewage and industrial wastewater, deteriorating water quality and ecological
57 environment (Pickett et al., 2011). Meanwhile, basin water cycle processes are
58 influenced by a combination of meteorological and subriver factors. It has been found
59 that urbanization has led to significant increases in runoff and peak flows in rivers
60 (Liu et al., 2018; Han et al., 2022) and has resulted in shorter runoff response times
61 (Anderson et al., 2022), which also exacerbates the intensity and frequency of
62 flooding in basins (De Niel and Willems, 2019; Blum et al., 2020). On the other hand,
63 the urbanization process leads to an increase in the amount of rainfall in the basin as
64 well as an increase in the frequency of extreme rainfall events (Shastri et al., 2015; Fu
65 et al., 2019; Yang et al., 2021), whereas in dryland inland river basins in arid zones
66 that are dependent on water resources for development, the impacts of urbanization on
67 the water cycle processes of the basins are still not clear, and they need to be explored

68 in depth the effects of urbanization on basin water cycle processes. Hence, study into
69 how human activities alter the features of river runoff and the water cycle within a
70 basin is essential for the prudent use and sustainable development of water resources.

71 Isotopes that are stable of hydrogen and oxygen are very useful tools for
72 investigating hydrological issues that are connected to river water and groundwater
73 sources (Fekete et al., 2006; Förstel and Hützen, 1983; Vystavna et al., 2021).
74 Researchers have been conducting studies using stable isotopes as tracers over the
75 course of the past few years in order to explore the impact that urbanization has had
76 on the water cycle. Urbanization has the potential to trigger and intensify convective
77 activity and warm-season rainfall in both urban areas and their surrounding regions
78 (Burian and Shepherd, 2005). Researchers generally agree that urbanization reduces
79 depressions on the underlying river, weakens water permeability and increases runoff.
80 At the same time, the lower roughness of the underlying river shortens the confluence
81 time (Guan et al., 2015; Oudin et al., 2018). Moreover, against the backdrop of swift
82 urbanization, the swift proliferation of urban regions has resulted in a sharp surge in
83 impermeable areas, alterations to regional microclimates, and the erection of a vast
84 number of infrastructures (including overpasses, subways, and so on), all of which
85 have significantly impacted the water cycle process in urban areas (Jacobson, 2011;
86 Westra et al., 2014). The complex connection between the permeable and
87 impermeable zones influences the river confluence processes (Bruwier et al., 2020).
88 The construction of urban water conservation projects, such as rubber dams and
89 pumping stations, also affects the confluence process of urban areas to a certain extent

90 (Zhu et al., 2021). Limited long-term and continuous monitoring has hampered
91 accurate depiction of urbanization's spatiotemporal effects on basin hydrology.
92 Furthermore, the scientific research till lacks sufficient research on arid regions that
93 heavily depend on mountain river runoff for sustenance and development.

94 Against the background of increasing urbanization, it is particularly important to
95 study the hydrological impacts of urbanization on basins and their corresponding
96 countermeasures, especially in arid inland river basins, where the impacts of human
97 activities in urban areas on rivers may be more prominent. Therefore, the Shiyang
98 River (SYR) basin, located in the inland arid zone of Northwest China, was used as an
99 example to study the impact of urbanization on the hydrology of the basin using the
100 stable isotope method. The following problems are proposed to be solved: (1) An
101 examination of the mechanisms underlying evaporation and infiltration of river water
102 within urban aquatic ecosystems; (2) Assessing the effects of urbanization on water
103 body connectivity through a comprehensive analysis; (3) The influence of
104 urbanization on the precipitation-runoff process is analyzed. This provides us with
105 essential information on how to maintain and manage the water resources found in
106 inland river basins, which is especially useful in light of the fact that the rate of
107 urbanization is growing.

108 **2 Observation Systems and Data**

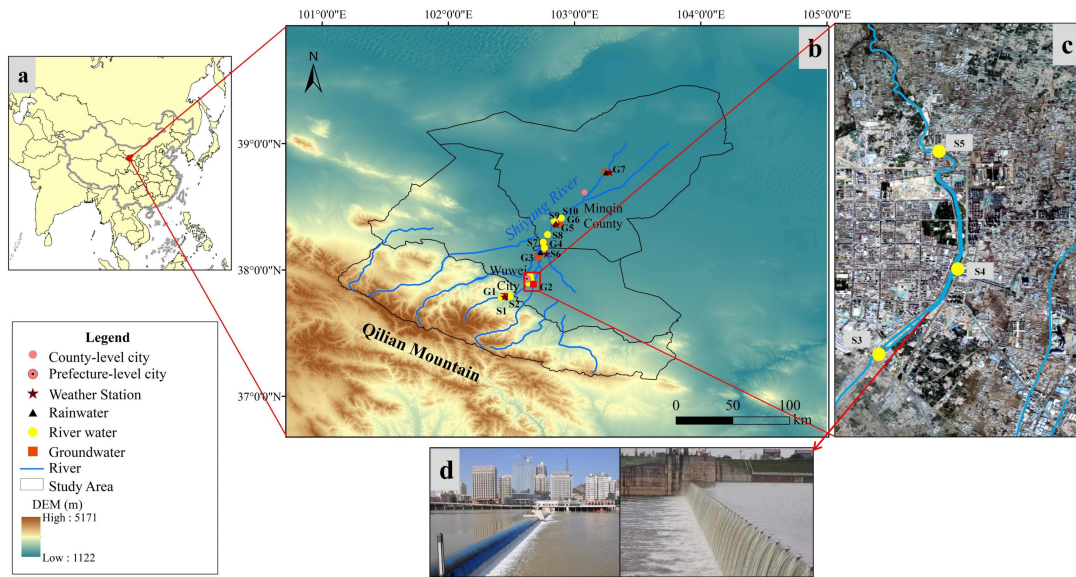
109 **2.1 Study Area**

110 The SYR basin is located in Gansu Province, China, to the east of the He-xi
111 Corridor. Its coordinates are $101^{\circ}41' \sim 104^{\circ}16'E$ and $36^{\circ}29' \sim 39^{\circ}27'N$. The SYR

112 basin is bounded to the west by the Wushaoling Mountain and to the north by the
113 foothills of the Qilian Mountain (Zhu et al., 2019). The basin in question is situated
114 within the continental temperate belt, characterized by a parched climate and diverse
115 topography. Annual precipitation hovers within the range of 100 to 600 mm, while
116 pan evaporation levels exhibit greater variability, ranging from 700 to 2600 mm
117 annually. The majesty of the Qilian Mountains is where the SYR begins its journey,
118 and the Qilian Mountains are the source of its eight main tributaries. The SYR is
119 principally supported by the convergence of precipitation, snowmelt, and glacier
120 runoff (Wei et al., 2013).

121 The Wuwei City is crossed by four important rivers, namely the Xiying, Zamu,
122 Huangyang and Jinta, which cover a catchment area of 3986 km². As the principal
123 water source for the entire region, the SYR basin is one of the most highly utilized
124 inland river basins in terms of water resource development and consumption
125 worldwide. The dams in the SYR basin are predominantly situated in close proximity
126 to the urbanized regions of Liangzhou District, located within Wuwei City. Liangzhou
127 District, situated in the middle of the basin, boasts of a relatively high population
128 density and a notable commercial concentration. At the turn of the millennium,
129 Wuwei City only boasted a paltry five landscape dams positioned on its rivers. As of
130 2019, this figure has surged dramatically, with a staggering total of 51 urban
131 landscape dams now gracing both urban and peri-urban areas of the city. These dams
132 are primarily composed of man-made landscape waterfalls and rubber dams, fulfilling
133 their core function of creating public landscape water bodies within the urban expanse.

134 (Zhu et al ., 2021).



135

136 Figure 1 (a) The location of the study area, (b) Comprehensive observation system for the study
137 area, (c) Urban river water sampling points (from Google Maps), (d) Common urban landscape
138 dams in SYR basin.

139 2.2 Sampling and data analysis

140 Since 2017, a comprehensive observation system has been established in the
141 SYR basin, and stable isotope observations and hydrometeorological observations
142 have been carried out on river water, shallow groundwater and rainfall. Continuous
143 sampling in the SYR basin was carried out from April 2017 to March 2021, different
144 water bodies were sampled, and we collected a total of 846 samples from 24 sampling
145 points (Table 1). The river sampling location ought to be selected such that it is
146 physically possible to go as close to the middle of the river as possible, with the goal
147 of minimizing the impact of areas with standing water and sewage. Artesian well
148 water was collected as groundwater samples at 7 sampling locations around the basin.
149 The automated weather station was used to measure meteorological factors such as

150 temperature and relative humidity while collecting precipitation samples. Water
 151 samples were sealed in high-density polyethylene bottles to avoid evaporation and
 152 leakage during transit and storage, precipitation samples were collected using weather
 153 station standard rain gauges. These samples were then frozen and wrapped with
 154 plastic tape.

155 Table 1 Basic information on precipitation, river water and groundwater sampling sites

Parameter	Sampling Point	Number	Sampling period	Collection Channels
Precipitation	P1, P2, P3, P4, P5,P6, P7,	387	Precipitation events	Rain tube collection
river Water	S1,S2,S3,S4,S5,S6, S7, S8, S9, S10	270	Monthly	Sampling in river water
Groundwater	G1, G2, G3, G4, G5, G6, G7	189	Monthly	Sampling from wells

156 Analysis of the water samples is conducted through liquid water isotope analysis
 157 utilizing the DLT-100 (Los Gatos Research, USA) in the Stable Isotope Laboratory at
 158 Northwest Normal University. Each water sample and isotope standard are injected
 159 six times in succession to assure reliable findings, with the first two injection values
 160 eliminated and the average of the last four injections used for final analysis, thereby
 161 avoiding any potential isotope analysis memory effect. The isotope measurements
 162 were denoted by the symbol " δ ," which indicates the deviation in thousandths from
 163 the Vienna Standard Mean Ocean Water:

$$164 \quad \delta_{\text{sample}}(\text{‰}) = \left[\left(\frac{R_s}{R_{v-smow}} \right) - 1 \right] \times 1000 \quad (1)$$

165 where R_s is the ratio of $^{18}\text{O}/^{16}\text{O}$ or $^2\text{H}/^1\text{H}$ in the collected sample, R_{v-smow} is the

166 ratio of $^{18}\text{O}/^{16}\text{O}$ or $^2\text{H}/^1\text{H}$ of the Vienna standard sample, and the analytical accuracy
167 of δD and $\delta^{18}\text{O}$ is $\pm 0.6\text{‰}$ and $\pm 0.2\text{‰}$, respectively.

168 **3 Methods**

169 **3.1 Calculation and indication of *d-excess***

170 Dansgaard (1964) introduced the concept of deuterium excess (*d-excess*) as the
171 difference in isotopic composition between global precipitation and the Vienna
172 Standard Mean Ocean Water (V_{SMOW}) reference water, which corresponds to a value of
173 10‰. This parameter reflects the average isotopic composition of air masses
174 associated with precipitation and is widely used to identify atmospheric source
175 regions (Deng et al., 2016). *d-excess* was proposed by Dansgaard (Dansgaard, 1964)
176 and is defined as:

$$177 \quad d\text{-excess} = \delta\text{D} - 8\delta^{18}\text{O} \quad (2)$$

178 **3.2 Calculation of evaporation losses of river water**

179 The losses of river water through evaporation and the resulting fluctuations in
180 water levels of rivers, lakes, and wetlands are key aspects of the terrestrial water cycle
181 that merit significant attention (Gammons et al., 2006; Hamilton et al., 2005).
182 Evaporation is the primary mechanism of water losses in the water cycle. For river
183 water in dry regions and urban river water that flows slowly due to manmade
184 constraints, evaporation cannot be ignored. Thus, it is vital to address the alteration of
185 urban landscape dam water caused by non-equilibrium isotope fractionation during
186 evaporation. The provided formula (3) can be used to estimate the rate of evaporative
187 water losses from the body of water in question (Skrzypek et al., 2015):

$$f = 1 - \left[\frac{(\delta - \delta^*)}{(\delta_0 - \delta^*)} \right]^{\frac{1}{m}} \quad (3)$$

188

189 The variables in the equation are as follows: f represents the ratio of water lost to
 190 evaporation, δ denotes the measured values of the water body located in the urban
 191 dam area of Wuwei City, situated in the middle reaches of the SYR and δ_0 represents
 192 the initial value of the hydrogen and oxygen stable isotope of the water body. It is
 193 widely assumed that the point of intersection between the local meteoric water line
 194 (LMWL) and the local evaporation line (LEL) represents the average isotopic
 195 composition of the input water body within the basin (Gibson et al., 2005). In the
 196 current investigation, the intersection point marked by $\delta^{18}\text{O} = -7.24\text{‰}$ and $\delta\text{D} =$
 197 -46.9‰ has been designated as the δ_0 value, while δ^* denotes the maximum isotope
 198 enrichment factor and m corresponds to the enrichment slope. The calculation of the
 199 above parameters in this paper is realized in Hydrocalculator software (Skrzypek et al.,
 200 2015) (<http://hydrocalculator.gskrzypek.com>). According to studies (Qian et al., 2007),
 201 it is more accurate to use $\delta^{18}\text{O}$ when calculating the evaporation losses ratio, so this
 202 study calculates the f value of SYR water using $\delta^{18}\text{O}$ value.

203 3.3 Periodic regression analysis and the mean residence time (MRT)

204 Seasonal fluctuations in $\delta^{18}\text{O}$ values were analyzed using periodic regression
 205 analysis to determine how these values changed over time. This method entailed
 206 fitting seasonal sine wave curves to annual $\delta^{18}\text{O}$ variations using least squares
 207 optimization (Rodgers et al., 2005):

$$\delta^{18}\text{O} = \delta^{18}\text{O}_{ave} + A \cdot [\cos(c \cdot t - \theta)] \quad (4)$$

208

209 The modelled $\delta^{18}O$ values and the mean weighted annual measured $\delta^{18}O_{ave}$
210 values were both utilized in the analysis of seasonal fluctuations in $\delta^{18}O$ levels.
211 Additionally, the measured $\delta^{18}O$ annual amplitude (A), the radial frequency of annual
212 fluctuations (c), and the time in days after the start of the sampling period (t) were
213 also considered in this analysis. Furthermore, the phase lag or time of the annual peak
214 $\delta^{18}O$ in radians (θ) was determined through this approach.

215 An exponential model was used for the purpose of estimating the mean residence
216 time (MRT). This model operates on the presumption that precipitation inputs quickly
217 mix with resident water. In order to do this, the following equation was used
218 (Maloszewski et al., 1983; Rodgers et al., 2005):

$$219 \quad MRT = c^{-1} \cdot \left[(A_{Z2} / A_{Z1})^{-2} - 1 \right]^{0.5} \quad (5)$$

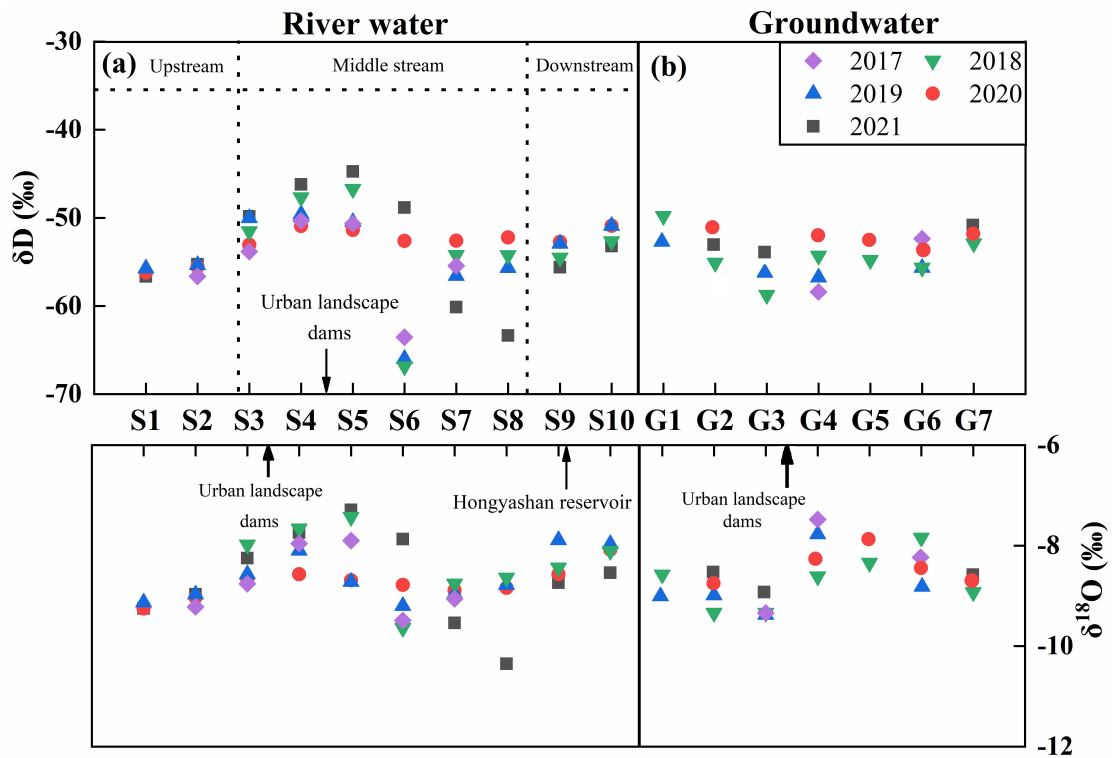
220 The amplitude of precipitation (A_{Z1}), the amplitude of the river water outputs
221 (A_{Z2}), and the radial frequency of the annual fluctuation (c) as defined in Eq. (4) were
222 taken into consideration to estimate the MRT.

223 **4 Results**

224 **4.1 Spatiotemporal distribution of isotopes in different water bodies**

225 The isotopes values of the river water in the SYR basin show a clear enrichment
226 from upstream to downstream when viewed from space. It is worth noting that
227 landscape dams and reservoirs in urban areas alter this pattern significantly, producing
228 markedly higher isotopic compositions of river water around such structures (Fig. 2).
229 To be more specific, the river water throughout the entire basin had average isotope
230 values that were lower than those of the sampling points in the dams region, which
231 had values that were greater (Table 2). In addition, the dams slowed the flow of the

232 river, this resulted in isotope enrichment of the river water. Notably, these values
 233 exhibit spatial and temporal variability, with the largest δD and $\delta^{18}O$ values observed
 234 in river water, and the lowest in groundwater.



235
 236 Figure 2 Longitudinal variation of δD and $\delta^{18}O$ in river water and groundwater in the SYR basin.

237 To be more specific, over the course of time, these values shift seasonally from
 238 spring to autumn (Table 2, Fig. 3). There was a range of values from -75.43‰ to
 239 -40.62‰ for the δD values of river water, with an average of -53.53‰. The $\delta^{18}O$
 240 values display a varied range, from -10.43‰ to -5.53‰, with an average of -8.54‰,
 241 whereas the *d-excess* values demonstrate variability ranging from 10.26‰ to 29.72‰,
 242 with 15.28‰ as the average value. A broad spectrum of δD values are observed
 243 during the summer season, ranging from -61.27‰ to -31.16‰, with an average
 244 -48.90‰. Meanwhile, $\delta^{18}O$ values fluctuate between -9.52‰ and -3.41‰, with an
 245 average -8.12‰. The phenomenon that was observed can be traced back primarily to

246 the aftereffects of the Hongyashan Reservoir built downstream. Because the reservoir
 247 has such a large capacity for water retention, it causes significant amounts of river
 248 water to evaporate in summer, which ultimately results in a discernible enrichment of
 249 the isotopic composition. In both river water and groundwater, δD and $\delta^{18}O$ showed
 250 significant seasonal variations (Fig. 3). Seasonal variations were more pronounced in
 251 river water than in groundwater, with river water showing the largest amplitude in
 252 spring and the smallest amplitude in fall, while groundwater showed closer
 253 amplitudes in all seasons, which also indicates that groundwater is less disturbed.

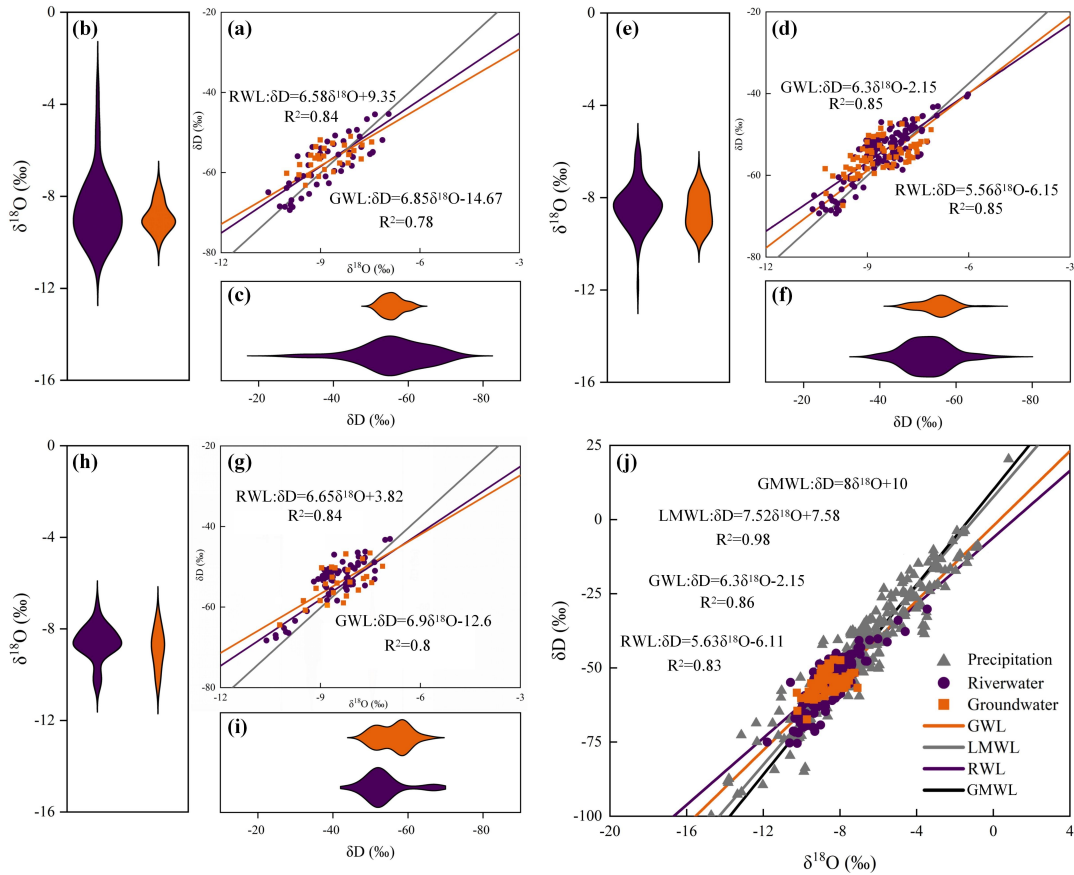
254 Table 2 Isotopic composition statistics of river water in SYR basin

Sampling Point	$\delta^{18}O$			δD			<i>d-excess</i>		
	Mean	Min.	Max.	Mean	Min.	Max.	Mean	Min.	Max.
S1	-9.35	-9.86	-9.06	-57.16	-59.46	-52.47	17.2	12.33	23.91
S2	-9.22	-10.02	-8.78	-56.62	-63.85	-10.02	16.46	15.53	19.28
S3	-7.74	-9.03	-7.75	-49.84	-50.76	-46.66	15.42	13.59	19.48
S4	-7.29	-8.79	-7.65	-46.22	-53.29	-46.26	14.9	11.01	18.03
S5	-7.43	-9.11	-5.53	-48.84	-56.66	-40.62	14.29	14.21	29.72
S6	-9.54	-10.43	-8.29	-60.14	-75.43	-54.40	14.31	10.26	17.62
S7	-9.04	-9.54	-8.21	-54.23	-70.04	-48.03	16.54	12.81	21.16
S8	-9.15	-10.35	-8.64	-56.37	-63.35	-52.22	16.84	14.56	19.54
S9	-8.41	-9.70	-6.02	-53.95	-65.33	-45.54	13.33	12.31	19.50
S10	-8.18	-8.84	-6.58	-51.92	-58.05	-45.39	13.48	12.21	21.72

256 **4.2 The Relationship between δD and $\delta^{18}O$ values**

257 As shown by the linear fitting equation $\delta D = 7.52\delta^{18}O + 7.58$, there is a significant
 258 linear positive correlation ($R^2 = 0.96$) between δD and $\delta^{18}O$ in atmospheric
 259 precipitation in the SYR basin (Fig. 3). It is clear that the slope (7.52) and intercept
 260 (7.58) of the local meteoric water line (LMWL) are smaller than the global meteoric
 261 water line (GMWL), which can be attributed to the basin's location in an inland arid
 262 region, where precipitation disturbances are less frequent and evaporative

263 fractionation of precipitation is stronger. On the other hand, compared with the slopes
264 of the LMWL, the slopes of the river water line (RWL) and the groundwater line
265 (GWL) are relatively close (Fig. 3), indicating that there is a strong hydraulic
266 connection between groundwater and river water in the SYR basin, and the slopes of
267 GWL and RWL show $GWL > RWL$ in all seasons, suggesting that the river water is
268 most affected by evaporation and groundwater is less affected by evaporation. In
269 addition, both river water and groundwater sampling points were distributed near the
270 LMWL, indicating that both river water and groundwater receive recharge from
271 precipitation. Overall, the H-O isotopic composition of river water samples from the
272 SYR showed a linear regression of $\delta D = 5.63\delta^{18}O - 6.11$, and the slope of RWL was
273 the largest in the autumn (slope = 6.65) and the smallest in the summer (slope = 5.56),
274 which indicated that the river water evaporated the weakest in the autumn and the
275 strongest in the summer.



276

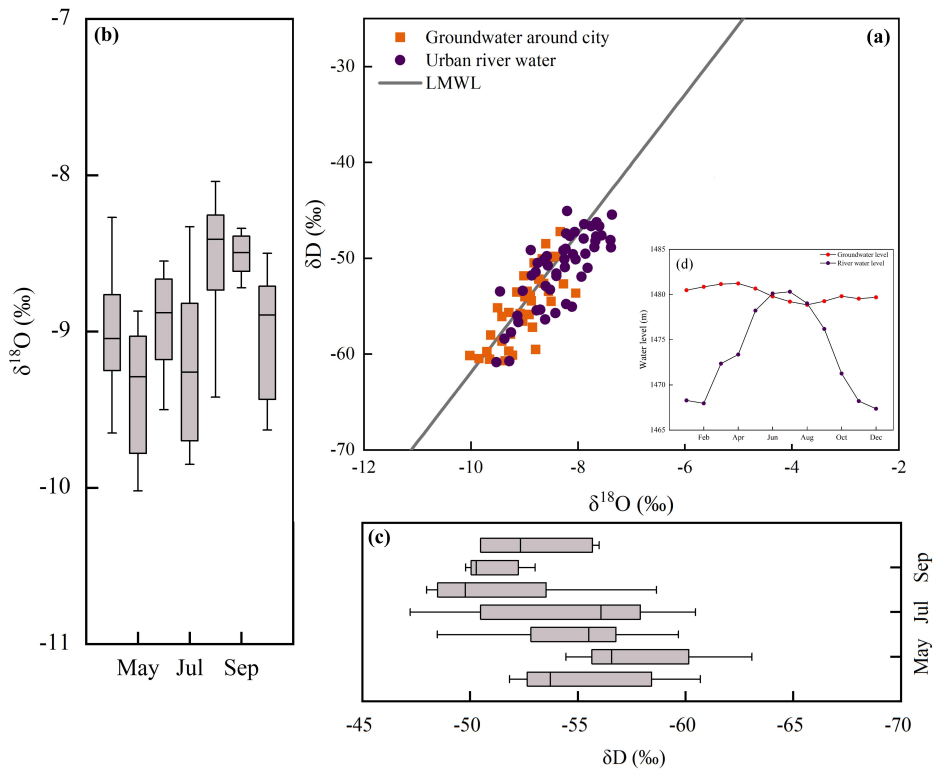
277 Figure 3 Relationship between δD and $\delta^{18}O$ in various water bodies in the SYR basin during
 278 different seasons (a,d,g represent spring, summer, autumn; j represent the comparison of RWL,
 279 GWL, LMWL and GMWL during the entire sampling period;b-c, e-f, h-i represent the
 280 distribution of δD and $\delta^{18}O$ in river water and groundwater in spring, summer and autumn).

281 Isotopic analysis of groundwater samples reveals a range of δD and $\delta^{18}O$ values
 282 spanning from -50.7‰ to -71.9‰ and from -7.23‰ to -10.4‰ , respectively.
 283 Moreover, the groundwater samples analyzed in the study displayed a linear
 284 regression of $\delta D = 6.3\delta^{18}O - 2.15$ ($R^2 = 0.86$). And it is interesting to note that
 285 groundwater also shows significant enrichment near the urban landscape dams (Fig.
 286 2), indicating that groundwater is also affected by evaporation, mainly because the
 287 Wuwei urban area is in the region of a large alluvial fan in front of the mountains, the
 288 sand and gravel aquifers are very permeable, and the depth of groundwater burial is

289 shallow, making the groundwater more susceptible to the effects of evaporation.

290 **4.3 Impact of urbanization on groundwater**

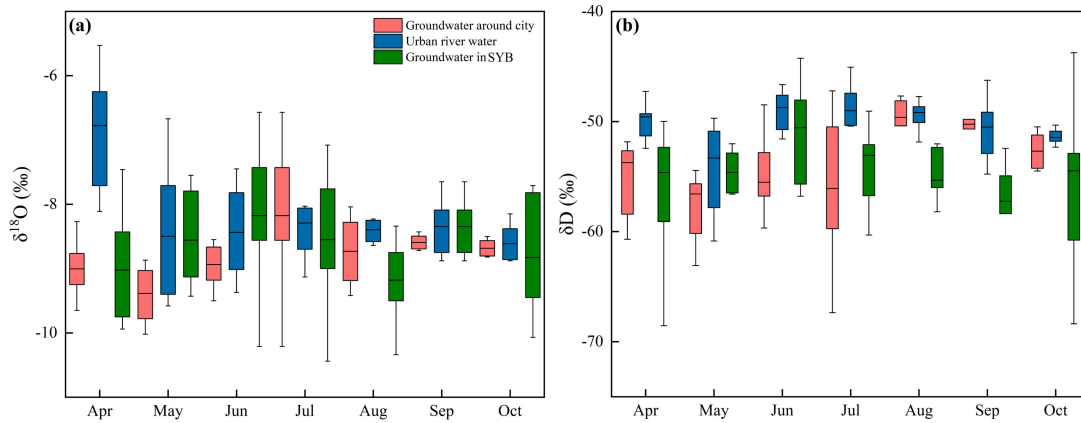
291 We compared monthly variations in isotopic values of groundwater near the city
292 with monthly variations in river water from a landscaped dam and found that the
293 monthly variations in groundwater near the city were closely related to river water
294 from a landscaped dam. The concentration of groundwater sampling sites near the city
295 near the sampling sites of the dam water indicates that the groundwater around the
296 city has similar isotopic signatures to the dam and river water (Fig. 4a). This suggests
297 that groundwater near the city is recharged by river water during the summer months.
298 In addition, we demonstrated this by comparing the data of the dam river water with
299 the groundwater level (Fig. 4). In addition, a portion of the groundwater sampling
300 sites around the city are located in the lower right corner of the LMWL, which
301 suggests that the groundwater around the city may also experience some degree of
302 evaporation.



303
 304 Figure 4 (a) Relationship between $\delta^{18}\text{O}$ and δD of groundwater around city and urban river water;
 305 (b) Monthly variations of $\delta^{18}\text{O}$ in groundwater around city; (c) Monthly variations of δD in
 306 groundwater around city; (d) Water levels in urban river water and groundwater around city.

307 In addition, we also compared and analyzed the changes of groundwater isotope
 308 values with those of groundwater around the city in the whole basin, and found that
 309 there was a close correlation between the changes of groundwater around the city and
 310 those of the river, while the other groundwater isotope values did not have a strong
 311 correlation with the river (Fig. 5). In the urban area, the mean values of δD and $\delta^{18}\text{O}$
 312 of the dammed river water were -7.49‰ and -48.31‰, respectively, while the mean
 313 values of δD and $\delta^{18}\text{O}$ of the groundwater around the city were -8.44‰ and -50.36‰,
 314 respectively, which indicated that the δD and $\delta^{18}\text{O}$ values of the groundwater around
 315 the city were similar to those of the river water in the dammed city. In addition, the
 316 isotopic mean values of δD and $\delta^{18}\text{O}$ of groundwater throughout the SYR basin were

317 -8.73‰ and -54.78‰, which are significantly different from the isotopic values of
318 river water in the urban dam.

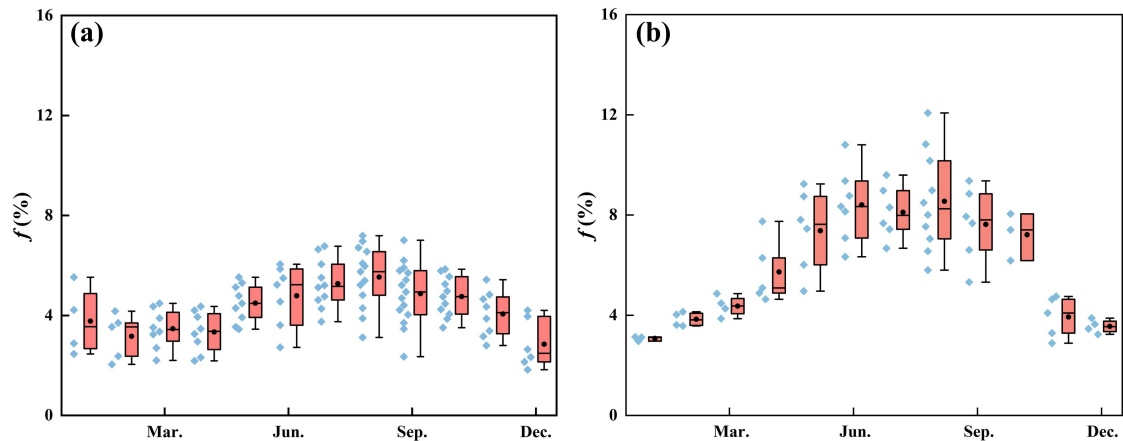


319
320 Figure 5 (a) Monthly variations of $\delta^{18}\text{O}$ in urban river water and groundwater around city, (b)
321 Monthly variations of δD in urban river water and groundwater around city.

322 4.4 Temporal and spatial variation of river water evaporation losses in the urban 323 area of Wuwei

324 In addition to being an essential part of the hydrological cycle, evaporation is
325 widely recognized as one of the most significant factors driving climate change in
326 semi-arid regions and in telluric ecosystems (Gibson et al., 2002; Gibson and Edwards,
327 2002). An obviously spatial and temporal fluctuation can be seen in the amount of
328 river water that is lost to evaporation in the upper mountain area as well as the
329 intermediate urban area of the SYR basin (Fig. 6). Analyzed from a time-varying
330 perspective, there is significant seasonal variation in river water evaporation losses
331 both in the upstream mountainous region and the midstream urban area of Wuwei,
332 with the highest rates occurring during summer and the lowest during winter (Fig.6).
333 Additionally, a spatial comparison reveals that river water evaporation losses in the
334 midstream urban area of Wuwei are significantly greater than those in the upstream

335 mountainous area.



336

337 Figure 6 Evaporation losses from river water in different areas of the SYR (a) Upper reaches

338 mountainous area, (b) Middle reaches urban areas.

339 Differences contributing to evaporation losses from the river in the upstream and

340 midstream urban areas can be explained mainly by the landscape characteristics of the

341 basin. In the upstream of the SYR higher vegetation cover and atmospheric humidity

342 in the mountainous areas result in weaker evaporation losses, while the midstream are

343 dominated by urban land, and urban landscapes increase the watershed area and slow

344 down the river, exacerbating evaporation losses from the river.

345 5 Discussion

346 5.1 Effects of Urbanization on the Rainfall-Runoff Process

347 Fig. 7 depicts the regression model of rainfall events in the SYR basin,

348 represented by a sine wave, and the fitting of river water $\delta^{18}\text{O}$ across the research

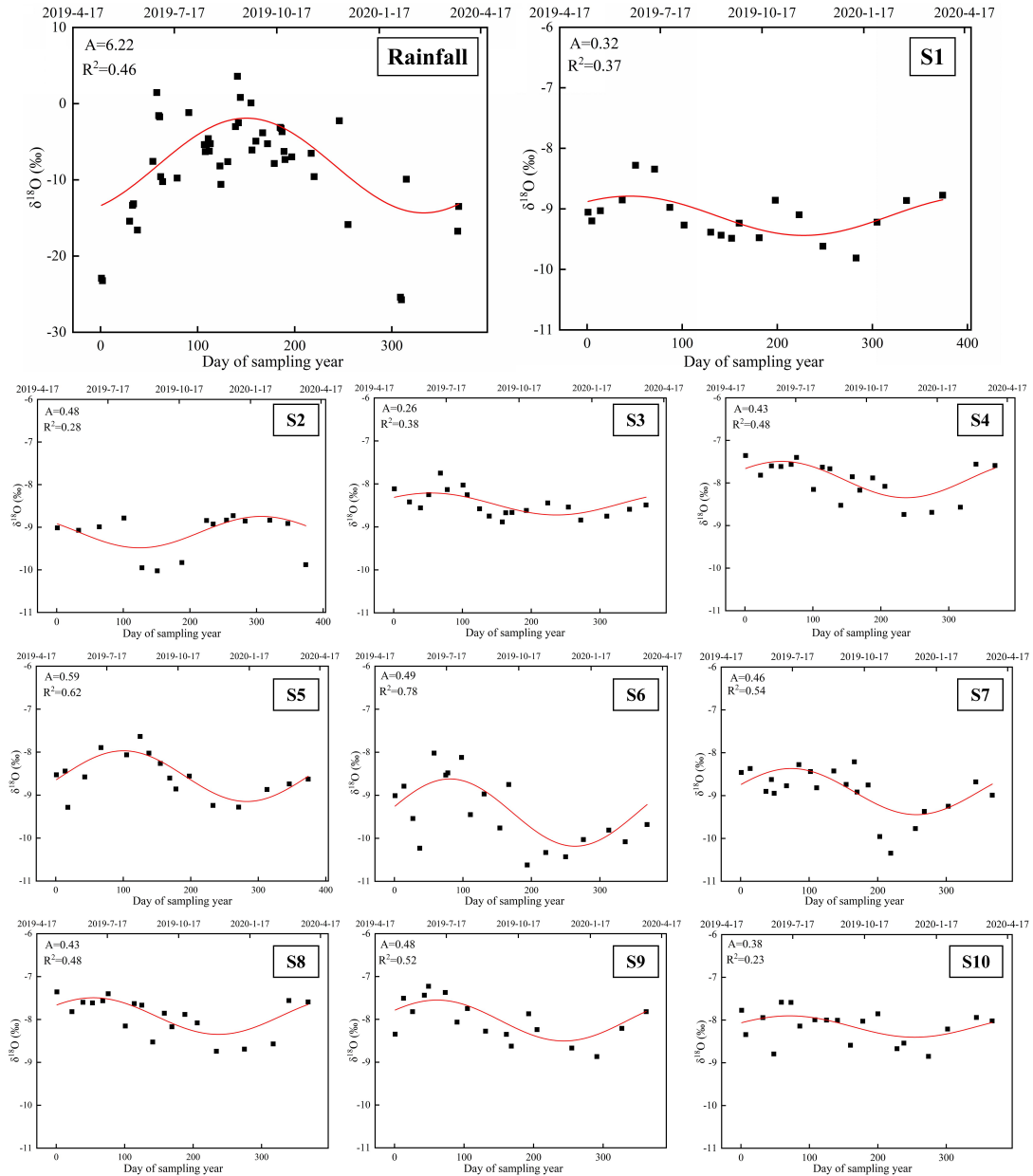
349 season. The $\delta^{18}\text{O}$ levels of precipitation reported in the SYR basin have an excellent

350 regularity ($R^2=0.46$) and a seasonal patterns trend that effectively depicts the nfluence

351 of the monsoon climate on the local environment (Zhu et al., 2019). Seasonal

352 variations are seen in the generally steady $\delta^{18}\text{O}$ and $\delta^{18}\text{O}$ values of the upstream water.

353 These results indicate that the predominant component of the river water is the
354 baseflow resulting from recent precipitation runoff. Throughout the duration of the
355 study, the majority of the lowest $\delta^{18}\text{O}$ values in the 10 river water sample points were
356 recorded during the winter, whilst the highest values were recorded during the
357 summer. These trends coincide with both the temporal variation of precipitation
358 isotopes in the SYR basin, indicating that precipitation input is the underlying cause
359 of isotope changes in river water. Nevertheless, variations in the isotopes of river
360 water differ in range across various regions within the SYR basin, with significant
361 variation in the degree of fit for the regression curve. The fitting degree of river water
362 in the upper and lower reaches is relatively low ($R^2=0.37$, $R^2=0.28$, $R^2=0.23$),
363 implying limited seasonal isotopic variability in these regions. The midstream river
364 water exhibits a notably higher degree of conformity as compared to its upstream and
365 downstream counterparts ($R^2=0.38$, $R^2=0.48$, $R^2=0.62$, $R^2=0.78$, $R^2=0.54$, $R^2=0.48$,
366 $R^2=0.52$). Moreover, the isotopic composition of river water throughout this area
367 exhibits notable cyclic variations.



368

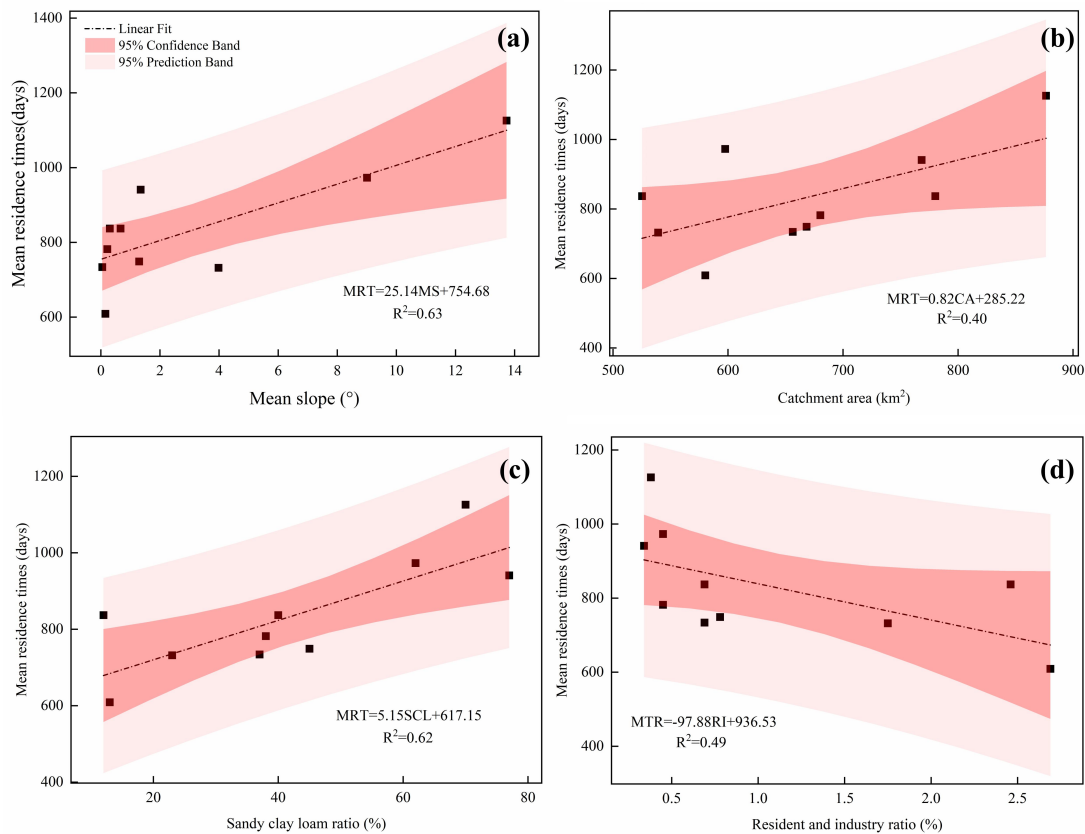
369 Figure 7 Fits the annual regression model of $\delta^{18}\text{O}$ in SYR basin precipitation and river water (time:
 370 2019/4/17—2020/4/23; S1-S10 are river water sampling points).

371 The reasons for differences in isotope periodicity in different regions may be
 372 attributed to local water management systems, topographic features and urban
 373 development. At points S1, S2, and S10, the correlation of model simulations was low,
 374 which could be attributed to the presence of Xiyang Reservoir in the upstream as well
 375 as Hongyashan Reservoir in the downstream (Sang et al., 2023), where seasonal

376 variations in the isotope values of the river water are interfered by the reservoir
377 dispatching activities. At points S3 to S5, the correlation of the model simulation is
378 higher, which is because in the middle reaches of the SYR basin, the expansion of
379 urban built-up areas leads to a significant increase in river runoff during the rainy
380 season, and according to the land use data, the land area of the towns in Wuwei City
381 has continued to increase by 134.38 km² from 2010 to 2018, resulting in the river
382 water showing a cyclical trend comparable to that of the precipitation. Since the 1950s,
383 in order to better utilize water resources, 13 small and medium-sized reservoirs with a
384 total storage capacity of 900,000 m³ were constructed during this period (Ma et al.,
385 2010), increasing the proportion of rainfall in the runoff constituents as a result of The
386 correlation of the model simulation is at a high level at points S6~S9, where, in
387 contrast to the high-elevation areas in the upper reaches, the terrain in the middle and
388 lower reaches of the SYR basin is relatively flat, mainly with cultivated land and
389 deserts, and is less disturbed by human activities (Sun et al., 2021), which further
390 reflects the responsiveness to recent precipitation inputs.

391 The Dunnett's test revealed a significant difference ($P < 0.05$) between the MRT
392 of the river and the annual magnitude of $\delta^{18}\text{O}$ of the river. We further investigated the
393 relationship between the estimated mean residence time and basin landscape features
394 such as topography (Fig. 8). Using the digital elevation model (DEM) to calculate the
395 mean slope of the SYR basin, we found that the mean residence time was also
396 strongly correlated with the mean basin slope ($R^2 = 0.63$), and that the upper reaches
397 of the SYR basin are mainly high-elevation mountainous areas, where the topography

398 is sloped, but where the vegetation cover is high and dominated by alpine meadows,
 399 subalpine scrub and Qinghai spruce (Zhang et al. 2023), the greater slope leads to a
 400 higher gravitational potential, which tends to result in a negative correlation with
 401 mean residence time (McGuire et al., 2005), which also contributes to the potentially
 402 higher MRT values in the upstream mountains. In our study, catchment area (CA) had
 403 a low correlation with MRT ($R^2 = 0.40$), and a weak relationship between catchment
 404 area and MRT has been observed in other studies (McGlynn et al., 2003; McGuire et
 405 al., 2005).



406
 407 Figure 8 Correlation between MRT and (a) mean slope of the basin, (b) catchment area, (c) sand
 408 clay loam ratio, and (d) percentage area of residential and industrial use in the basin, with 95%
 409 Confidence and Prediction bands.

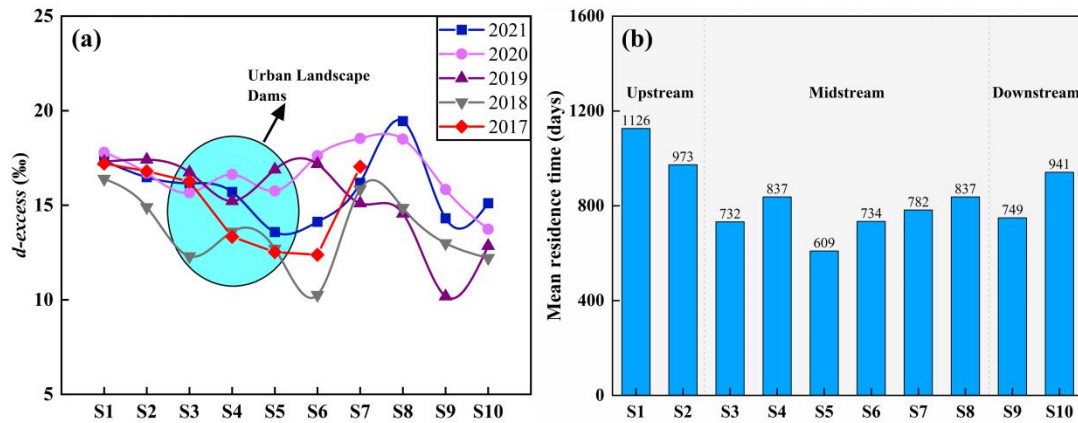
410 Soil is an important component of basin hydrology, and the physical properties

411 of soil, such as water-holding capacity and pore space distribution, have an important
412 influence on the response to precipitation in the basin and the sand-clay-loam soil
413 ratio is used here to investigate the possible relationship with MRT. The results
414 showed that the content of sand clay loam ratio showed a strong positive correlation
415 with MRT ($R^2=0.62$). Wuwei City is located in the pre-mountain flood-fan belt, and
416 the soil is dominated by sandy soil (Zhang et al., 2023), which is loose in texture, has
417 good permeability and good water retention properties, and is mainly used for
418 agricultural cultivation. Its good permeability increases the vertical movement of
419 water and the length of flow paths, leading to a longer MRT. There is a strong
420 negative correlation between the MRT and the ratios of resident and industrial areas
421 (RI) ($R^2=0.49$), which also indicates that as urbanization progresses, with the increase
422 of urban land, this undoubtedly leads to a significant shortening of the MRT. However,
423 the MRT in the mid-river urban area is not much shorter as compared to the
424 downstream, which may be attributed to the fact that the mid-river The large number
425 of landscape dams constructed in the urban areas, currently 51 urban landscape dams
426 have been built in the peri-urban areas of Wuwei City, and the considerable number of
427 landscape dams may have counteracted the impact of the urban land use, resulting in a
428 lengthening of the MRT in the middle reaches as well.

429 **5.2 Effects of Water Conservancy Projects in Urban Areas on Isotope Dynamics**

430 Recent studies have suggested that the development of dam-reservoir systems
431 may result in river fragmentation and modifications in flow regimes in terms of their
432 volume, frequency, and duration (Négrel et al., 2016; Murgulet et al., 2016; Peñas and

433 Barquín, 2019; Maavara et al., 2020). Furthermore, chemical-containing nutrient
434 migration, such as phosphorus, may occur during sediment movement, resulting in
435 widespread eutrophication problems (Yang et al., 2007; Duan et al., 2019). As of 2019,
436 a total of 51 urban landscape dams, primarily consisting of artificial landscape
437 waterfalls and rubber dams, have been constructed in and around Wuwei city (Zhu et
438 al., 2021). In the metropolitan coast of Wuwei, many landscape dams have led to
439 isotopic enrichment in river water. This damping effect has been observed in
440 numerous dammed rivers across the globe, including the Rio Grande in the
441 southwestern United States (Vitvar et al., 2007) and the Ebro River in Spain (Négre
442 et al., 2016), as evidenced by isotopic tracers. In the metropolitan coast of Wuwei, a
443 number of landscape dams have led to the enrichment of isotopic tracers in the river
444 water. The results indicate that the δD and $\delta^{18}O$ levels of the river water at the outflow
445 of Wuwei City are greater than those at the inflow (Fig. 2). Moreover, the influence of
446 evaporation on isotopic composition should not be overlooked, as it can lead to a
447 decrease in *d-excess* values (Peng et al., 2012). Consistent with previous studies
448 (Wang et al., 2019), we observed that the *d-excess* of influent water was higher than
449 that of urban river water (Fig. 9). This observation further supports the accumulation
450 of heavy H-O isotopes in the river waters of the dam areas, as shown in Fig. 9a. In
451 contrast, due to the confluence of tributaries prior to the S7 sampling point, the river
452 water has lower isotopic values, resulting in elevated *d-excess* values between S6 and
453 S8.



454

455 Figure 9 (a) The longitudinal variation of the river water *d-excess* of the SYR, (b) The longitudinal

456 variation of the river water MRT of the SYR.

457 5.3 Effects of Urbanization on the Water Cycle of basins

458 Localized microclimates in urban areas allow for changes in precipitation and

459 evapotranspiration processes, while urbanization alters the pristine subriver,

460 complicating water cycle processes in the basin (Jacobson, 2011; Westra et al., 2014;

461 Oudin et al., 2018). In terms of the impact on runoff, it is mainly reflected in the

462 increase of river impermeability due to urbanization, the land use area of Wuwei

463 urban land increased by about 134.38 km² from 2010 to 2018, which greatly

464 weakened the infiltration process in urban areas, and the rainfall runoff process

465 simulated by sinusoidal cyclic regression method showed that there were significant

466 differences in the river metro in different parts of the SYR basin, and that the middle

467 reaches of the river had the highest degree of urbanization, and the time of the metro

468 was the shortest, which further increases the contribution of rainfall to runoff.

469 Regarding the effect of urbanization on evapotranspiration, a large number of dams

470 were constructed on the SYR and flowed through the urban area of Wuwei, causing

471 significant evapotranspiration losses, in addition, these landscape dams also led to

472 hydrogen and oxygen isotope enrichment, and the numerous reservoirs that were
473 constructed for the construction and development of the city (Ma et al., 2010), and
474 these reservoirs also contributed to a significant evapotranspiration loss effect, which
475 has been previously confirmed in our study was also confirmed (Sang et al., 2023).
476 On the other hand, our study found that the isotopic compositions and trends of urban
477 nearshore groundwater were similar to those of river water, which suggests that there
478 is a close correlation between urban nearshore groundwater and river water, and that
479 the difference in water levels between river water and groundwater may be the main
480 reason for river recharge of urban nearshore groundwater (Fig. 4d). In the rainy
481 season, the river level gradually rises, which decreases the difference between the
482 water levels of urban nearshore groundwater and river water, and the river water
483 recharges the groundwater, and in the dry season, the river level decreases, and the
484 urban nearshore groundwater, which is buried at a shallow depth, in turn recharges the
485 river.

486 In addition, the growth of urbanization has had a dramatic impact on the water
487 environment in cities, where water problems occur frequently (Giri and Qiu, 2016;
488 Ma et al., 2022). Urbanization has increased impervious rivers such as parking lots,
489 rooftops, roads, and sidewalks, leading to increased runoff, which creates additional
490 pathways for pollutants to be transported from landscapes to water bodies (Ren et al.,
491 2014; Wilson and Weng, 2010; Nolan et al., 2023). On the other hand, agricultural
492 activities have increased some of the fertilizers, pesticides, herbicides and dairy
493 manure in the farmland into the nearest water bodies, which can directly and

494 indirectly affect will reduce water quality (Yu et al., 2013). The SYR basin in the
495 Northwest Arid Zone is an inland river basin with the highest development intensity
496 and the sharpest conflict between water supply and demand in the region. The
497 Liangzhou district in the central part of the SYR basin is the most densely populated
498 artificial oasis with the largest scale of water demand in the entire basin. Our previous
499 study found that direct discharge of industrial and community domestic wastewater
500 into the river led to deterioration of river water quality around the SYR basin (Ma et
501 al., 2021). In addition agricultural activities have less impact on the upper reaches of
502 the SYR and relatively more impact on the middle and lower reaches , and the
503 application of nitrogen-based fertilizers during agricultural cultivation is the main
504 cause of high NH_4^+ and NO_3^- concentrations in the area (Ma et al., 2021), which may
505 also lead to increased salinity and accelerated eutrophication of the river, threatening
506 the safety of the basin's water environment. Overall, human activities (urbanization)
507 may alter the water cycle processes inherent in inland river basins, and the
508 implications of such changes need to be further explored.

509 **6 Conclusions**

510 In this study, we investigated the hydrometeorological and isotopic data of the
511 Shiyang River basin from 2017 to 2021, and our investigations showed that
512 urbanization had a significant impact on the water cycle of the basin. The results
513 showed that the isotopic values of the river water showed a significant enrichment
514 from upstream to downstream, but facilities such as landscape dams and reservoirs in
515 the urban area significantly altered this natural pattern, and the isotopic values of the

516 river water in the urban area ($\delta D=-48.31\text{‰}$; $\delta^{18}\text{O}=-7.49\text{‰}$) were higher than those of
517 the natural river water ($\delta D=-55.77\text{‰}$; $\delta^{18}\text{O}=-8.98\text{‰}$), and landscape dams aggravated
518 the evaporation losses of river water, due to the increase of urban land area, which
519 accelerated the rainfall-runoff conversion process, the residence time of river water in
520 different regions of the Shiyang River basin had obvious differences, and the MRT
521 from the upstream to the downstream showed a fluctuating downward process, which
522 was shortened from 1,126 days in the upstream to 941 days in the downstream, and
523 the MRT was mainly controlled by the basin's landscape features. In addition, there
524 was a strong relationship between the isotopic composition of the reservoir and the
525 surrounding groundwater. Overall, urbanization has a profound impact on the
526 hydrological system of the basin, and the results of this study can provide some
527 references for future research on urbanization and the water cycle, and improve our
528 understanding of the hydrological processes of basin in arid zones.

529 **Acknowledgements**

530 This research was financially supported by the National Natural Science
531 Foundation of China (41971036, 41867030).

532 **Author contributions statement**

533 Rui Li: Writing-Original draft preparation; Guofeng Zhu: Writing-Reviewing and
534 Editing; Siyu Lu: Methodology; Liyuan Sang and Gaojia Meng: Data processing and
535 Experiment; Longhu Chen and Yinying Jiao: Methodology and visualization;
536 Qinqin Wang : Visualization;

537 **Data availability Statement**

538 The isotopic data that support the findings of this study are openly available in
539 Zhu, Guofeng (2022), “Stable water isotope monitoring network of different water
540 bodies in SYR Basin, a typical arid river in China”, Mendeley Data, V1, doi:
541 10.17632/vhm44t74sy.1. The source of soil data comes from the Harmonized World
542 Soil Database (HWSD) constructed by the Food and Agriculture Organization of the
543 United Nations (FAO) and the International Institute for Applied Systems (IIASA) on
544 2009. The land-use and land-cover change data of the Shiyang River Basin were
545 obtained from Chinese Academy of Sciences, the data centre of resources and
546 environmental science (<http://www.resdc.cn>).

547 **Competing Interests**

548 We undersigned declare that this manuscript entitled “Effects of Urbanization on
549 the water cycle in the SYR Basin: Based on stable isotope method” is original, has not
550 been published before and is not currently being considered for publication elsewhere.

551 The authors declare that they have no known competing financial interests or
552 personal relationships that could have appeared to influence the work reported in this
553 paper.

554 **Reference**

555 Anderson, B. J., Slater, L. J., Dadson, S. J., Blum, A. G., and Prosdocimi, I.:
556 Statistical Attribution of the Influence of Urban and Tree Cover Change on
557 Streamflow: A Comparison of Large Sample Statistical Approaches, *Water
558 Resources Research*, 58, e2021WR030742,
559 <https://doi.org/10.1029/2021WR030742>, 2022.

560 Asano, Y., Uchida, T., and Ohte, N.: Residence times and flow paths of water in steep
561 unchannelled catchments, Tanakami, Japan, *Journal of Hydrology*, 261, 173–192,
562 [https://doi.org/10.1016/S0022-1694\(02\)00005-7](https://doi.org/10.1016/S0022-1694(02)00005-7), 2002.

563 Baker, A.: Land Use and Water Quality, in: *Encyclopedia of Hydrological Sciences*,
564 edited by: Anderson, M. G. and McDonnell, J. J., John Wiley & Sons, Ltd,
565 Chichester, UK, hsa195, <https://doi.org/10.1002/0470848944.hsa195>, 2005.

566 Bhaskar, A. S. and Welty, C.: Analysis of subriver storage and streamflow generation
567 in urban basins, *Water Resour. Res.*, 51, 1493–1513,
568 <https://doi.org/10.1002/2014WR015607>, 2015.

569 Blum, A. G., Ferraro, P. J., Archfield, S. A., and Ryberg, K. R.: Causal Effect of
570 Impervious Cover on Annual Flood Magnitude for the United States,
571 *Geophysical Research Letters*, 47, e2019GL086480,
572 <https://doi.org/10.1029/2019GL086480>, 2020.

573 Bruwier, M., Maravat, C., Mustafa, A., Teller, J., Piroton, M., Erpicum, S.,
574 Archambeau, P., and Dewals, B.: Influence of urban forms on river flow in urban
575 pluvial flooding, *Journal of Hydrology*, 582, 124493,
576 <https://doi.org/10.1016/j.jhydrol.2019.124493>, 2020.

577 Burian, S. J. and Shepherd, J. M.: Effect of urbanization on the diurnal rainfall pattern
578 in Houston, *Hydrol. Process.*, 19, 1089–1103, <https://doi.org/10.1002/hyp.5647>,
579 2005.

580 Caldwell, P. V., Sun, G., McNulty, S. G., Cohen, E. C., and Moore Myers, J. A.:
581 Impacts of impervious cover, water withdrawals, and climate change on river

582 flows in the conterminous US, *Hydrol. Earth Syst. Sci.*, 16, 2839–2857,
583 <https://doi.org/10.5194/hess-16-2839-2012>, 2012.

584 Chen, G., Li, X., Liu, X., Chen, Y., Liang, X., Leng, J., Xu, X., Liao, W., Qiu, Y., Wu,
585 Q., and Huang, K.: Global projections of future urban land expansion under
586 shared socioeconomic pathways, *Nat Commun.*, 11, 537,
587 <https://doi.org/10.1038/s41467-020-14386-x>, 2020.

588 Dansgaard, W.: Stable isotopes in precipitation, *Tellus*, 16, 436–468,
589 <https://doi.org/10.1111/j.2153-3490.1964.tb00181.x>, 1964.

590 De Niel, J. and Willems, P.: Climate or land cover variations: what is driving observed
591 changes in river peak flows? A data-based attribution study, *Hydrol. Earth Syst.*
592 *Sci.*, 23, 871–882, <https://doi.org/10.5194/hess-23-871-2019>, 2019.

593 Deng, K., Yang, S., Lian, E., Li, C., Yang, C., and Wei, H.: Three Gorges Dam alters
594 the Changjiang (Yangtze) river water cycle in the dry seasons: Evidence from
595 H-O isotopes, *Science of The Total Environment*, 562, 89–97,
596 <https://doi.org/10.1016/j.scitotenv.2016.03.213>, 2016.

597 Duan, W., Hanasaki, N., Shiogama, H., Chen, Y., Zou, S., Nover, D., Zhou, B., and
598 Wang, Y.: Evaluation and Future Projection of Chinese Precipitation Extremes
599 Using Large Ensemble High-Resolution Climate Simulations, *Journal of Climate*,
600 32, 2169–2183, <https://doi.org/10.1175/JCLI-D-18-0465.1>, 2019.

601 Fekete, B. M., Gibson, J. J., Aggarwal, P., and Vörösmarty, C. J.: Application of
602 isotope tracers in continental scale hydrological modeling, *Journal of Hydrology*,
603 330, 444–456, <https://doi.org/10.1016/j.jhydrol.2006.04.029>, 2006.

604 Flörke, M., Schneider, C., and McDonald, R. I.: Water competition between cities and
605 agriculture driven by climate change and urban growth, *Nat Sustain*, 1, 51–58,
606 <https://doi.org/10.1038/s41893-017-0006-8>, 2018.

607 Förstel, H. and Hützen, H.: Oxygen isotope ratios in German groundwater, *Nature*,
608 304, 614–616, <https://doi.org/10.1038/304614a0>, 1983.

609 Fu, X., Yang, X., and Sun, X.: Spatial and Diurnal Variations of Summer Hourly
610 Rainfall Over Three Super City Clusters in Eastern China and Their Possible
611 Link to the Urbanization, *JGR Atmospheres*, 124, 5445–5462,
612 <https://doi.org/10.1029/2019JD030474>, 2019.

613 Gammons, C. H., Poulson, S. R., Pellicori, D. A., Reed, P. J., Roesler, A. J., and
614 Petrescu, E. M.: The hydrogen and oxygen isotopic composition of precipitation,
615 evaporated mine water, and river water in Montana, USA, *Journal of Hydrology*,
616 328, 319–330, <https://doi.org/10.1016/j.jhydrol.2005.12.005>, 2006.

617 Gessner, M. O., Hinkelmann, R., Nützmann, G., Jekel, M., Singer, G., Lewandowski,
618 J., Nehls, T., and Barjenbruch, M.: Urban water interfaces, *Journal of Hydrology*,
619 514, 226–232, <https://doi.org/10.1016/j.jhydrol.2014.04.021>, 2014.

620 Gibson, J. J., Edwards, T. W. D., Birks, S. J., St Amour, N. A., Buhay, W. M.,
621 McEachern, P., Wolfe, B. B., and Peters, D. L.: Progress in isotope tracer
622 hydrology in Canada, *Hydrol. Process.*, 19, 303–327,
623 <https://doi.org/10.1002/hyp.5766>, 2005.

624 Gibson, J. J. and Edwards, T. W. D.: Regional water balance trends and
625 evaporation-transpiration partitioning from a stable isotope survey of lakes in

626 northern Canada: REGIONAL WATER BALANCE USING STABLE
627 ISOTOPES, *Global Biogeochem. Cycles*, 16, 10-1-10-14,
628 <https://doi.org/10.1029/2001GB001839>, 2002.

629 Gibson, J. J., Prepas, E. E., and McEachern, P.: Quantitative comparison of lake
630 throughflow, residency, and catchment runoff using stable isotopes: modelling
631 and results from a regional survey of Boreal lakes, *Journal of Hydrology*, 2002.

632 Gillefalk, M., Tetzlaff, D., Hinkelmann, R., Kuhlemann, L.-M., Smith, A., Meier, F.,
633 Maneta, M. P., and Soulsby, C.: Quantifying the effects of urban green space on
634 water partitioning and ages using an isotope-based ecohydrological model,
635 *Hydrol. Earth Syst. Sci.*, 25, 3635–3652,
636 <https://doi.org/10.5194/hess-25-3635-2021>, 2021.

637 Giri, S. and Qiu, Z.: Understanding the relationship of land uses and water quality in
638 Twenty First Century: A review, *Journal of Environmental Management*, 173,
639 41–48, <https://doi.org/10.1016/j.jenvman.2016.02.029>, 2016.

640 Grimm, N. B., Faeth, S. H., Golubiewski, N. E., Redman, C. L., Wu, J., Bai, X., and
641 Briggs, J. M.: Global Change and the Ecology of Cities, *Science*, 319, 756–760,
642 <https://doi.org/10.1126/science.1150195>, 2008.

643 Guan, M., Sillanpää, N., and Koivusalo, H.: Storm runoff response to rainfall pattern,
644 magnitude and urbanization in a developing urban catchment: Storm Runoff
645 Response to Rainfall Pattern, Magnitude and Urbanization, *Hydrol. Process.*,
646 n/a-n/a, <https://doi.org/10.1002/hyp.10624>, 2015.

647 Hamilton, S. K., Bunn, S. E., Thoms, M. C., and Marshall, J. C.: Persistence of
648 aquatic refugia between flow pulses in a dryland river system(Cooper Creek,
649 Australia), *Limnol. Oceanogr.*, 50, 743–754,
650 <https://doi.org/10.4319/lo.2005.50.3.0743>, 2005.

651 Han, S., Slater, L., Wilby, R. L., and Faulkner, D.: Contribution of urbanisation to
652 non-stationary river flow in the UK, *Journal of Hydrology*, 613, 128417,
653 <https://doi.org/10.1016/j.jhydrol.2022.128417>, 2022.

654 Jacobson, C. R.: Identification and quantification of the hydrological impacts of
655 imperviousness in urban catchments: A review, *Journal of Environmental*
656 *Management*, 92, 1438–1448, <https://doi.org/10.1016/j.jenvman.2011.01.018>,
657 2011.

658 Liu, J., Shen, Z., and Chen, L.: Assessing how spatial variations of land use pattern
659 affect water quality across a typical urbanized basin in Beijing, China,
660 *Landscape and Urban Planning*, 176, 51–63,
661 <https://doi.org/10.1016/j.landurbplan.2018.04.006>, 2018.

662 Ma, H., Zhu, G., Zhang, Y., Sang, L., Wan, Q., Zhang, Z., Xu, Y., and Qiu, D.: Ion
663 migration process and influencing factors in inland river basin of arid area in
664 China: a case study of Shiyang River Basin, *Environ Sci Pollut Res*, 28,
665 56305–56318, <https://doi.org/10.1007/s11356-021-14484-3>, 2021.

666 Ma, J., Pan, F., Chen, L., Edmunds, W. M., Ding, Z., He, J., Zhou, K., and Huang, T.:
667 Isotopic and geochemical evidence of recharge sources and water quality in the

668 Quaternary aquifer beneath Jinchang city, NW China, *Applied Geochemistry*, 25,
669 996–1007, <https://doi.org/10.1016/j.apgeochem.2010.04.006>, 2010.

670 Ma, X., Li, N., Yang, H., and Li, Y.: Exploring the relationship between urbanization
671 and water environment based on coupling analysis in Nanjing, East China,
672 *Environ Sci Pollut Res*, 29, 4654–4667,
673 <https://doi.org/10.1007/s11356-021-15161-1>, 2022.

674 Maavara, T., Chen, Q., Van Meter, K., Brown, L. E., Zhang, J., Ni, J., and Zarfl, C.:
675 River dam impacts on biogeochemical cycling, *Nat Rev Earth Environ*, 1,
676 103–116, <https://doi.org/10.1038/s43017-019-0019-0>, 2020.

677 Małoszewski, P., Rauert, W., Stichler, W., and Herrmann, A.: Application of flow
678 models in an alpine catchment area using tritium and deuterium data, *Journal of*
679 *Hydrology*, 66, 319–330, [https://doi.org/10.1016/0022-1694\(83\)90193-2](https://doi.org/10.1016/0022-1694(83)90193-2), 1983.

680 Martin, K. L., Hwang, T., Vose, J. M., Coulston, J. W., Wear, D. N., Miles, B., and
681 Band, L. E.: basin impacts of climate and land use changes depend on magnitude
682 and land use context, *Ecohydrology*, 10, e1870, <https://doi.org/10.1002/eco.1870>,
683 2017.

684 McDonough, L. K., Santos, I. R., Andersen, M. S., O’Carroll, D. M., Rutledge, H.,
685 Meredith, K., Oudone, P., Bridgeman, J., Gooddy, D. C., Sorensen, J. P. R.,
686 Lapworth, D. J., MacDonald, A. M., Ward, J., and Baker, A.: Changes in global
687 groundwater organic carbon driven by climate change and urbanization, *Nat*
688 *Commun*, 11, 1279, <https://doi.org/10.1038/s41467-020-14946-1>, 2020.

689 McGlynn, B., McDonnell, J., Stewart, M., and Seibert, J.: On the relationships
690 between catchment scale and streamwater mean residence time, *Hydrol. Process.*,
691 17, 175–181, <https://doi.org/10.1002/hyp.5085>, 2003.

692 McGuire, K. J., McDonnell, J. J., Weiler, M., Kendall, C., McGlynn, B. L., Welker, J.
693 M., and Seibert, J.: The role of topography on catchment-scale water residence
694 time: CATCHMENT-SCALE WATER RESIDENCE TIME, *Water Resour. Res.*,
695 41, <https://doi.org/10.1029/2004WR003657>, 2005.

696 Murgulet, D., Murgulet, V., Spalt, N., Douglas, A., and Hay, R. G.: Impact of
697 hydrological alterations on river-groundwater exchange and water quality in a
698 semi-arid area: Nueces River, Texas, *Science of The Total Environment*, 572,
699 595–607, <https://doi.org/10.1016/j.scitotenv.2016.07.198>, 2016.

700 Négrel, P., Petelet-Giraud, E., and Millot, R.: Tracing water cycle in regulated basin
701 using stable $\delta^{18}\text{O}$ – $\delta^2\text{H}$ isotopes: The Ebro river basin (Spain), *Chemical Geology*,
702 422, 71–81, <https://doi.org/10.1016/j.chemgeo.2015.12.009>, 2016.

703 Nolan, T. M., Reynolds, L. J., Sala-Comorera, L., Martin, N. A., Stephens, J. H.,
704 O’Hare, G. M. P., O’Sullivan, J. J., and Meijer, W. G.: Land use as a critical
705 determinant of faecal and antimicrobial resistance gene pollution in riverine
706 systems, *Science of The Total Environment*, 871, 162052,
707 <https://doi.org/10.1016/j.scitotenv.2023.162052>, 2023.

708 Oudin, L., Salavati, B., Furusho-Percot, C., Ribstein, P., and Saadi, M.: Hydrological
709 impacts of urbanization at the catchment scale, *Journal of Hydrology*, 559,
710 774–786, <https://doi.org/10.1016/j.jhydrol.2018.02.064>, 2018.

711 Peñas, F. J. and Barquín, J.: Assessment of large-scale patterns of hydrological
712 alteration caused by dams, *Journal of Hydrology*, 572, 706–718,
713 <https://doi.org/10.1016/j.jhydrol.2019.03.056>, 2019.

714 Peng, T.-R., Huang, C.-C., Wang, C.-H., Liu, T.-K., Lu, W.-C., and Chen, K.-Y.:
715 Using oxygen, hydrogen, and tritium isotopes to assess pond water's contribution
716 to groundwater and local precipitation in the pediment tableland areas of
717 northwestern Taiwan, *Journal of Hydrology*, 450–451, 105–116,
718 <https://doi.org/10.1016/j.jhydrol.2012.05.021>, 2012.

719 Pickett, S. T. A., Cadenasso, M. L., Grove, J. M., Boone, C. G., Groffman, P. M.,
720 Irwin, E., Kaushal, S. S., Marshall, V., McGrath, B. P., Nilon, C. H., Pouyat, R.
721 V., Szlavecz, K., Troy, A., and Warren, P.: Urban ecological systems: Scientific
722 foundations and a decade of progress, *Journal of Environmental Management*, 92,
723 331–362, <https://doi.org/10.1016/j.jenvman.2010.08.022>, 2011.

724 Qian, H., Dou, Y., Li, X.J., Yang, B.C., and Zhao, Z.H.: Changes of $\delta^{18}\text{O}$ and δD
725 along Dousitu River and its indication of river water evaporation. *Hydrogeol.*
726 *Eng. Geol.* 34 (1), 107–112,
727 <https://doi.org/10.16030/j.cnki.issn.1000-3665.2007.01.024>, 2007.

728 Ren, L., Cui, E., and Sun, H.: Temporal and spatial variations in the relationship
729 between urbanization and water quality, *Environ Sci Pollut Res*, 21,
730 13646–13655, <https://doi.org/10.1007/s11356-014-3242-8>, 2014.

731 Rodgers, P., Soulsby, C., Waldron, S., and Tetzlaff, D.: Using stable isotope tracers to
732 assess hydrological flow paths, residence times and landscape influences in a

733 nested mesoscale catchment, *Hydrol. Earth Syst. Sci.*, 9, 139–155,
734 <https://doi.org/10.5194/hess-9-139-2005>, 2005.

735 Salvadore, E., Bronders, J., and Batelaan, O.: Hydrological modelling of urbanized
736 catchments: A review and future directions, *Journal of Hydrology*, 529, 62–81,
737 <https://doi.org/10.1016/j.jhydrol.2015.06.028>, 2015.

738 Sang, L., Zhu, G., Xu, Y., Sun, Z., Zhang, Z., and Tong, H.: Effects of Agricultural
739 Large-And Medium-Sized Reservoirs on Hydrologic Processes in the Arid
740 Shiyang River Basin, Northwest China, *Water Resources Research*, 59,
741 e2022WR033519, <https://doi.org/10.1029/2022WR033519>, 2023.

742 Shastri, H., Paul, S., Ghosh, S., and Karmakar, S.: Impacts of urbanization on Indian
743 summer monsoon rainfall extremes, *J. Geophys. Res. Atmos.*, 120, 496–516,
744 <https://doi.org/10.1002/2014JD022061>, 2015.

745 Skrzypek, G., Mydłowski, A., Dogramaci, S., Hedley, P., Gibson, J. J., and Grierson,
746 P. F.: Estimation of evaporative loss based on the stable isotope composition of
747 water using Hydrocalculator, *Journal of Hydrology*, 523, 781–789,
748 <https://doi.org/10.1016/j.jhydrol.2015.02.010>, 2015.

749 Sun, G., Caldwell, P. V., and McNulty, S. G.: Modelling the potential role of forest
750 thinning in maintaining water supplies under a changing climate across the
751 conterminous United States: Response of Water Yield to Forest Thinning and
752 Climate Change, *Hydrol. Process.*, 29, 5016–5030,
753 <https://doi.org/10.1002/hyp.10469>, 2015.

754 Sun, G. and Lockaby, B. G.: Water Quantity and Quality at the Urban-Rural Interface,
755 in: Urban-Rural Interfaces, edited by: Laband, D. N., Lockaby, B. G., and
756 Zipperer, W. C., American Society of Agronomy, Soil Science Society of
757 America, Crop Science Society of America, Inc., Madison, WI, USA, 29–48,
758 <https://doi.org/10.2136/2012.urban-rural.c3>, 2012.

759 Sun, Z., Zhu, G., Zhang, Z., Xu, Y., Yong, L., Wan, Q., Ma, H., Sang, L., and Liu, Y.:
760 Identifying river water evaporation loss of inland river basin based on
761 evaporation enrichment model, *Hydrological Processes*, 35, e14093,
762 <https://doi.org/10.1002/hyp.14093>, 2021.

763 Talma, S, Woodborne, S. and Lorentz, S.: South African Contribution to the Rivers
764 CRP, 2012.

765 UN-Habitat: World cities report 2020 : the value of sustainable urbanization,
766 UN-Habitat, Nairobi, Kenya, 377 pp., 2020.

767 United Nations Department of Economic and Social Affairs: World Urbanization
768 Prospects 2018: Highlights, United Nations,
769 <https://doi.org/10.18356/6255ead2-en>, 2019.

770 Vitvar, T., Aggarwal, P. K., and Herczeg, A. L.: Global network is launched to
771 monitor isotopes in rivers, *Eos Trans. AGU*, 88, 325–326,
772 <https://doi.org/10.1029/2007EO330001>, 2007.

773 Vystavna, Y., Harjung, A., Monteiro, L. R., Matiatos, I., and Wassenaar, L. I.: Stable
774 isotopes in global lakes integrate catchment and climatic controls on evaporation,
775 *Nat Commun*, 12, 7224, <https://doi.org/10.1038/s41467-021-27569-x>, 2021.

776 Wang, B., Zhang, H., Liang, X., Li, X., and Wang, F.: Cumulative effects of cascade
777 dams on river water cycle: Evidence from hydrogen and oxygen isotopes,
778 *Journal of Hydrology*, 568, 604–610,
779 <https://doi.org/10.1016/j.jhydrol.2018.11.016>, 2019.

780 Wei, W., Shi, P., Zhou, J., Feng, H., Wang, X., and Wang, X.: Environmental
781 suitability evaluation for human settlements in an arid inland river basin: A case
782 study of the Shiyang River Basin, *J. Geogr. Sci.*, 23, 331–343,
783 <https://doi.org/10.1007/s11442-013-1013-y>, 2013.

784 Westra, S., Fowler, H. J., Evans, J. P., Alexander, L. V., Berg, P., Johnson, F.,
785 Kendon, E. J., Lenderink, G., and Roberts, N. M.: Future changes to the intensity
786 and frequency of short-duration extreme rainfall, *Rev. Geophys.*, 52, 522–555,
787 <https://doi.org/10.1002/2014RG000464>, 2014.

788 Wilson, C. and Weng, Q.: Assessing river Water Quality and Its Relation with Urban
789 Land Cover Changes in the Lake Calumet Area, Greater Chicago, *Environmental*
790 *Management*, 45, 1096–1111, <https://doi.org/10.1007/s00267-010-9482-6>, 2010.

791 Wing, O. E. J., Bates, P. D., Smith, A. M., Sampson, C. C., Johnson, K. A., Fargione,
792 J., and Morefield, P.: Estimates of present and future flood risk in the
793 conterminous United States, *Environ. Res. Lett.*, 13, 034023,
794 <https://doi.org/10.1088/1748-9326/aaac65>, 2018.

795 Yang, L., Ni, G., Tian, F., and Niyogi, D.: Urbanization Exacerbated Rainfall Over
796 European Suburbs Under a Warming Climate, *Geophysical Research Letters*, 48,
797 e2021GL095987, <https://doi.org/10.1029/2021GL095987>, 2021.

798 Yang, S. L., Zhang, J., and Xu, X. J.: Influence of the Three Gorges Dam on
799 downstream delivery of sediment and its environmental implications, Yangtze
800 River, *Geophys. Res. Lett.*, 34, L10401, <https://doi.org/10.1029/2007GL029472>,
801 2007.

802 Yu, D., Shi, P., Liu, Y., and Xun, B.: Detecting land use-water quality relationships
803 from the viewpoint of ecological restoration in an urban area, *Ecological*
804 *Engineering*, 53, 205–216, <https://doi.org/10.1016/j.ecoleng.2012.12.045>, 2013.

805 Zhang, W., Wan, Q., Zhu, G., and Xu, Y.: Distribution of soil organic carbon and
806 carbon sequestration potential of different geomorphic units in Shiyang river
807 basin, China, *Environ Geochem Health*, 45, 4071–4086,
808 <https://doi.org/10.1007/s10653-022-01472-w>, 2023.

809 Zhu, G., Guo, H., Qin, D., Pan, H., Zhang, Y., Jia, W., and Ma, X.: Contribution of
810 recycled moisture to precipitation in the monsoon marginal zone: Estimate based
811 on stable isotope data, *Journal of Hydrology*, 569, 423–435,
812 <https://doi.org/10.1016/j.jhydrol.2018.12.014>, 2019.

813 Zhu, G., Sang, L., Zhang, Z., Sun, Z., Ma, H., Liu, Y., Zhao, K., Wang, L., and Guo,
814 H.: Impact of landscape dams on river water cycle in urban and peri-urban areas
815 in the Shiyang River Basin: Evidence obtained from hydrogen and oxygen
816 isotopes, *Journal of Hydrology*, 602, 126779,
817 <https://doi.org/10.1016/j.jhydrol.2021.126779>, 2021.